J Shoulder Elbow Surg (2021) 30, 237–249

ELSEVIER

Journal of Shoulder and Elbow Surgery

www.elsevier.com/locate/ymse

Three-dimensional computed tomography analysis of pathologic correction in total shoulder arthroplasty based on severity of preoperative pathology

Eric T. Ricchetti, MD[a,*], Bong-Jae Jun, PhD[b], Yuxuan Jin, MS[c], Vahid Entezari, MD, MMSc[a], Thomas E. Patterson, PhD[a], Kathleen A. Derwin, PhD[b], Joseph P. Iannotti, MD, PhD[a]

[a]*Department of Orthopaedic Surgery, Orthopedic and Rheumatologic Institute, Cleveland Clinic, Cleveland, OH, USA*
[b]*Department of Biomedical Engineering, Lerner Research Institute, Cleveland Clinic, Cleveland, OH, USA*
[c]*Department of Quantitative Health Sciences, Cleveland Clinic, Cleveland, OH, USA*

Background: The purpose of this study was to quantify correction of glenoid deformity and humeral head alignment in anatomic total shoulder arthroplasty as a function of preoperative pathology (modified Walch classification) and glenoid implant type in a clinical cohort using 3-dimensional computed tomography (CT) analysis.

Methods: Patients undergoing anatomic total shoulder arthroplasty with a standard glenoid (SG) (n = 110) or posteriorly stepped augmented glenoid (AG) (n = 62) component were evaluated with a preoperative CT scan and a postoperative CT scan within 3 months of surgery. Glenoid version, inclination, and medial-lateral (ML) joint line position, as well as humeral head alignment, were assessed on both CT scans, with preoperative-to-postoperative changes analyzed relative to pathology and premorbid anatomy based on the modified Walch classification and glenoid implant type.

Results: On average, correction to the premorbid ML joint line position was significantly less in type A2 glenoids than in type A1 glenoids (–2.3 ± 2.1 mm vs. 1.1 ± 0.9 mm, $P < .001$). Correction to premorbid version was not different between type B2 glenoids with AG components and type A1 glenoids with SG components (–1.7° ± 6.6° vs. –1.0° ± 4.0°, $P = .57$), and the premorbid ML joint line position was restored on average in both groups (0.3 ± 1.6 mm vs. 1.1 ± 0.9 mm, $P = .006$). Correction to premorbid version was not different between type B3 glenoids with AG components and type A1 glenoids with SG components (–0.6° ± 5.1° vs. –1.0° ± 4.0°, $P = .72$), but correction relative to the premorbid ML joint line position was significantly less in type B3 glenoids with AG components than in type A1 glenoids with SG components (–2.2 ± 2.1 mm vs. 1.1 ± 0.9 mm, $P < .001$). Postoperative humeral glenoid alignment was not different in any group comparisons.

Discussion: In cases with posterior glenoid bone loss and retroversion (type B2 or B3 glenoids), an AG component can better correct retroversion and the glenoid ML joint line position compared with an SG component, with correction to premorbid version comparable to a type A1 glenoid with an SG component. However, restoration of the premorbid ML joint line position may not always be possible with SG or AG components in cases with more advanced central glenoid bone loss (type A2 or B3 glenoids). Further follow-up is needed to determine the clinical consequences of these findings.

Institutional Review Board (IRB) approval was obtained for this study (Cleveland Clinic IRB study nos. 12-997, 13-652, and 14-789).

*Reprint requests: Eric T. Ricchetti, MD, Department of Orthopaedic Surgery, Orthopedic and Rheumatologic Institute, Cleveland Clinic, 9500 Euclid Ave, Mail Code A40, Cleveland, OH 44195, USA.
E-mail address: ricchee@ccf.org (E.T. Ricchetti).

https://doi.org/10.1016/j.jse.2020.07.033

Level of evidence: Level II; Prospective Cohort Design; Treatment Study

Keywords: Walch classification; glenohumeral osteoarthritis; computed tomography; three-dimensional; total shoulder arthroplasty; glenoid component

Primary glenohumeral osteoarthritis can progress to involve substantial glenoid bone loss in both central (type A2 glenoid) and posterior (type B2 or B3 glenoid) wear patterns, as defined by the original and modified Walch classifications.[1,21,48] Although both wear patterns result in medialization of the joint line, posterior glenoid bone loss is also associated with increased pathologic glenoid retroversion and posterior subluxation of the humeral head.[1,21,48] Prior studies have demonstrated that correction of more advanced glenoid retroversion, posterior humeral head subluxation, and joint line medialization owing to posterior glenoid bone loss may not always be possible in anatomic total shoulder arthroplasty (TSA) with routine surgical techniques, such as eccentric glenoid reaming. However, these prior studies have been limited to mostly cadaveric and computer simulation investigations.[6,13,20,32] Clinically, this combination of pathology when seen in the type B2 or B3 glenoid has been associated with worse outcomes following anatomic TSA, including increased rates of glenoid component loosening.[8,49] This finding may relate to the difficulty in correcting these pathologies at the time of surgery, as joint line medialization and postoperative glenoid retroversion have been independently associated with glenoid component radiolucency and/or loosening.[6,10,15,16,18,47] Although type B2 and B3 glenoids both demonstrate these pathologic characteristics, these glenoid types do show distinct morphologic differences that served as an impetus for modifications of the Walch classification and may impact surgical decision making and clinical outcomes. In the type B2 glenoid, posterior glenoid wear leads to a biconcave appearance with high glenoid retroversion and posterior humeral head subluxation, whereas in the type B3 glenoid, a mono-concave appearance with high retroversion, joint line medialization, and more variable posterior humeral head subluxation results from posterior wear and further central erosion.[1,5,21,48]

Owing to the limits of routine surgical techniques, other surgical options have been recommended to address more advanced posterior glenoid bone loss in these settings, including reverse TSA and augmented glenoid (AG) components.[15,26,29,38] Posteriorly augmented glenoid components have been developed for use in anatomic TSA with preclinical and early clinical studies showing promising results and the ability to correct glenoid pathology not possible with standard glenoid (SG) components.[11,15,22,39,40,45,51] However, postoperative imaging evaluation in clinical series has been limited to plain radiographs, which do not accurately assess postoperative implant position and pathologic correction from the preoperative state,[2-4,17,28,33,37,52] and cadaveric and computer simulation studies of pathologic corrections may not accurately reflect what is achievable in a clinical environment. More recent studies have demonstrated the use of postoperative 3-dimensional (3D) computed tomography (CT) to accurately measure postoperative implant position following anatomic TSA to assess the efficacy of 3D CT preoperative surgical planning tools and patient-specific instrumentation (PSI),[24,25] but surgical correction relative to preoperative pathology has not been specifically evaluated. Therefore, minimal data are currently available accurately assessing pathologic correction and implant position following anatomic TSA based on preoperative pathology and glenoid component type in a clinical patient population.

The purpose of this study was to quantify correction of glenoid deformity and humeral head alignment as a function of preoperative pathology (modified Walch classification) and implant type (SG vs. AG component) in a clinical cohort using 3D CT analysis. We hypothesized that there may be limits to certain surgical corrections with current implants based on the modified Walch classification and the severity of preoperative pathologic measurements, particularly glenoid version and medial-lateral (ML) joint line position. In type A1 and A2 glenoids with SG components, we hypothesized that the postoperative glenoid component ML joint line position would be associated with the severity of preoperative joint line medialization. In type B2 and B3 glenoids, we hypothesized that postoperative glenoid component version and ML joint line position would be associated with the preoperative Walch classification, glenoid component type, and severity of preoperative retroversion and joint line medialization.

Materials and methods

One hundred seventy-two patients with advanced glenohumeral osteoarthritis and an intact rotator cuff who underwent anatomic TSA with a standard (n = 110) (Global Anchor Peg Glenoid; DePuy Synthes, Raynham, MA, USA) or posteriorly stepped augmented (n = 62) (Global STEPTECH Anchor Peg Glenoid; DePuy Synthes) polyethylene anchor peg glenoid component were prospectively evaluated with preoperative CT (CT1) and postoperative CT within 3 months of surgery (CT2). The mean age at surgery was 63 ± 8 years (range, 43-90 years). Patients were enrolled from 3 institutional review board–approved studies originally investigating the use of 3D preoperative surgical planning and PSI in primary anatomic TSA.[24,25]

Three 1.0-mm-diameter, radiopaque tantalum marker beads (RSA Biomedical, Umeå, Sweden) were implanted in the peripheral pegs of each glenoid component at surgery for component detection on postoperative CT, as previously described.[24,25] All surgical procedures were performed by 1 of 2 staff shoulder surgeons (E.T.R. or J.P.I.), each with extensive experience using 3D preoperative surgical planning. The glenoid implant that best restored premorbid anatomy as defined by the glenoid vault model was chosen between the standard and augmented components in each case, with glenoid version typically corrected to $\leq$–10° and inclination corrected to $\leq$+10° and with the least amount of bone removal to maintain or restore the glenoid ML joint line position.[24] The glenoid vault model, a standardized 3D model of the normal glenoid vault, has been shown to be a highly consistent and conserved shape across normal individuals and is predictive of premorbid glenoid version, inclination, and ML joint line position when placed into a pathologic glenoid.[7,12,21,35,42,44] The AG component was used in patients with moderate to severe posterior glenoid bone loss or retroversion (Walch type C1 or C2 glenoid or moderate to severe Walch type B2 or B3 glenoid), whereas the SG component was used in patients without glenoid bone loss (Walch type A1 glenoid), symmetrical glenoid bone loss (Walch type A2 glenoid), or mild anterior or posterior glenoid bone loss requiring <10° of version correction (Walch type B1, mild Walch type B2 or B3, or mild Walch type D glenoid).

CT scans were obtained with a 0.6-mm slice thickness and the following acquisition parameters: 140 kV (peak), 300 mA with dose modulation on, 0.6 mm of collimation, 512 × 512 matrix, no gantry tilt, and field of view that included the entire scapula. Preoperative CT scans were reconstructed using a standard filtered backprojection algorithm, and postoperative CT scans were reconstructed using an iterative metal artifact reduction algorithm (iMAR; Siemens, Munich, Germany) in the axial plane with a medium smooth kernel (B40).[30,46] The patient was scanned supine with the operative arm at the side of the body. CT DICOM (Digital Imaging and Communications in Medicine) images were imported into 3D imaging software (OrthoVis Shoulder Research; Cleveland Clinic, Cleveland, OH, USA) for analysis, as previously described.[7,9,12,14,17,21,23,25,27,35,36,42-44,50,53] To quantify correction of glenoid pathology between preoperative (CT1) and postoperative (CT2) scans, the bony scapula of each scan was registered to the scapular coordinate system of CT1, as previously described.[14,23,31,34]

Anatomic measurements on preoperative CT

Preoperative CT scans (CT1) were used to measure premorbid and pathologic anatomy, as previously described.[7,9,12,14,17,21,23,25,27,35,36,42-44,50,53] Pathologic glenoid version, inclination, and ML joint line position were measured 3-dimensionally with respect to the scapular coordinate system (Fig. 1). Humeral head alignment was measured in the axial plane (anteroposterior [AP]) with respect to the scapular coordinate system, both relative to the scapular axis as humeral scapular alignment (HSA-AP) and relative to the glenoid axis as humeral glenoid alignment (HGA-AP) (Fig. 2). Both measures were expressed as a percentage of humeral head diameter. The glenoid vault model was then placed into the glenoid of each CT scan to estimate the patient's premorbid glenoid anatomy (version, inclination, and ML joint line position), as previously described (Fig. 1).[7,12,21,35,42,44] Preoperative joint line medialization was defined as the difference between the pathologic ML joint line position and the premorbid ML joint line position (CT1 – Vault).

Preoperative glenoid morphology was classified by the modified Walch classification (type A1, A2, B1, B2, B3, C1, C2, or D) through blinded consensus reads by 2 staff shoulder surgeons (E.T.R. and J.P.I.), as previously described.[1,21] There were 48 type A1, 18 type A2, 8 type B1, 53 type B2, 35 type B3, 3 type C1, 3 type C2, and 4 type D glenoids in the cohort.

Implant measurements on postoperative CT

Postoperative CT scans (CT2) were used to measure glenoid and humeral head component positions, as previously described.[14,23-25,36] The locations of both components were automatically detected and displayed as overlaid digital templates based on (1) 4 radiopaque markers (3 tantalum markers and center-peg metal pin) in the glenoid component pegs and (2) volumetric center fit of the humeral head component. Correct position of the digital templates was confirmed or adjusted if needed following automatic detection. Glenoid component version, inclination, and ML joint line position, as well as humeral head component alignment (HSA-AP and HGA-AP), were measured similarly to the preoperative CT scan data (Fig. 2).

Statistical methods

The low frequency of type B1, C1, C2, and D glenoids precluded meaningful statistical comparisons of these cases. Therefore, they were excluded from analysis, leaving 154 cases (48 type A1, 18 type A2, 53 type B2, and 35 type B3) for comparison. Preoperative-to-postoperative changes were determined for glenoid version, inclination, and ML joint line relative to pathologic (CT2 – CT1) and premorbid (CT2 – Vault) anatomy and analyzed based on the modified Walch classification (type A1, A2, B2, or B3) and glenoid component type (SG or AG component). The frequencies of cases with type A1 and A2 glenoids, all of which received SG components, achieving correction of $\geq$–1 mm, $\geq$–3 mm, or $\geq$–5 mm of the premorbid ML joint line position were calculated. Similarly, the frequencies of cases with type B2 and B3 glenoids receiving either SG or AG components and achieving correction of premorbid version and ML joint line position at 3 different thresholds were calculated: (1) within 5° of premorbid version and 1 mm of the premorbid joint line, (2) within 10° of premorbid version and 3 mm of the premorbid joint line, or (3) within 15° of premorbid version and 5 mm of the premorbid joint line. Recommendations on surgical correction vary in the literature, with no guidelines for surgical correction of the glenoid ML joint line and/or glenoid version that have been shown to result in a clinically significant difference in outcome. Therefore, the current thresholds were chosen to create standardized regions for statistical evaluation; they were also chosen based on their use for analysis in prior studies of 3D preoperative surgical planning[19,24,25] and prior studies suggesting clinical relevance.[6,10,15,16,18,47]

Preoperative-to-postoperative changes relative to pathologic (CT2 – CT1) and premorbid (CT2 – Vault) anatomy were compared between select groups using 2-sample *t* tests. Postoperative (CT2) humeral head alignment was also compared between select groups using 2-sample *t* tests. Type A1 glenoids with SG components were considered a control group for comparison,

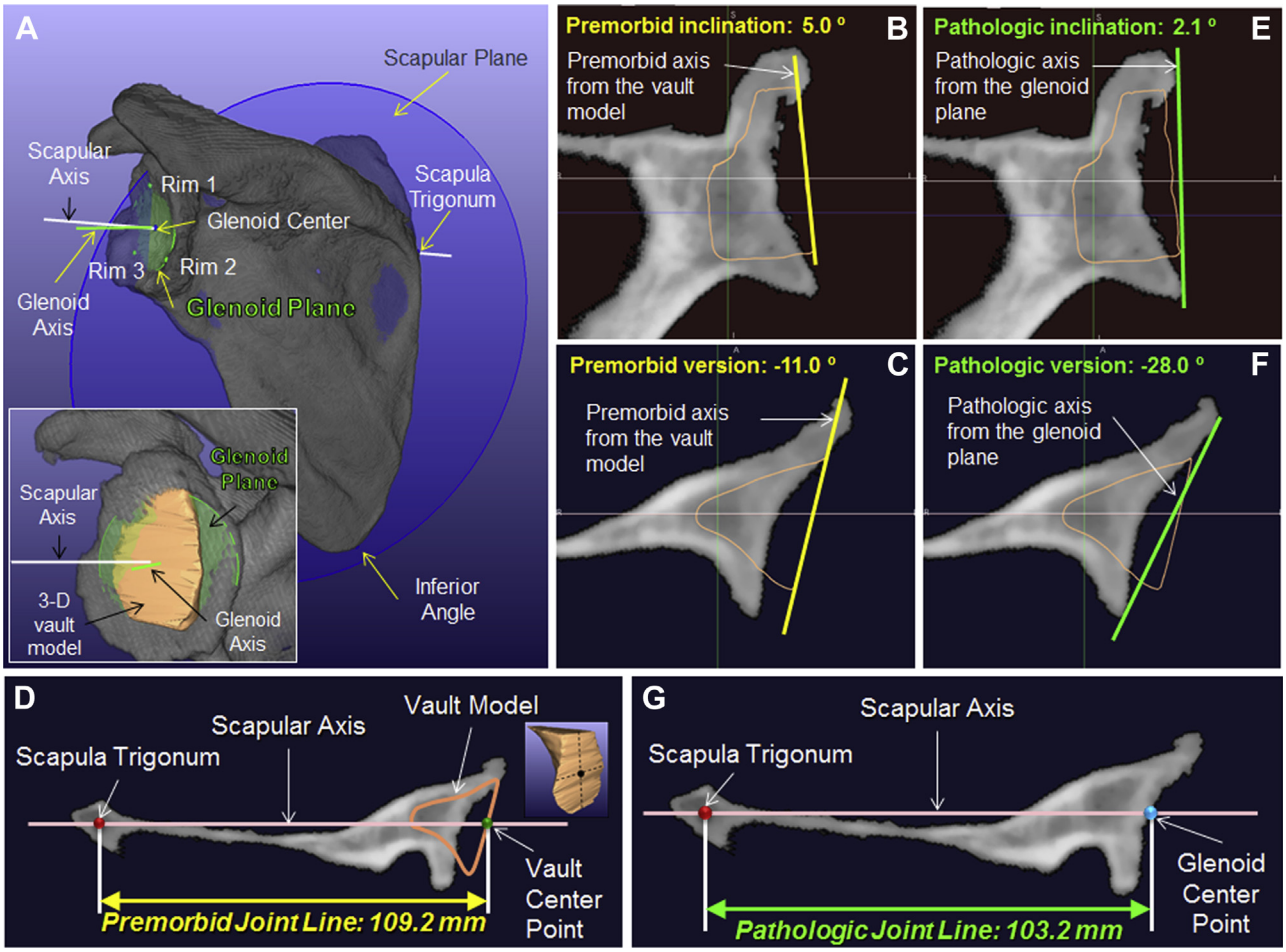

Figure 1 (**A**) The scapular plane is defined using the glenoid center point, inferior angle of the scapula, and scapula trigonum. The glenoid plane is defined using 3 representative points placed on the surface of the glenoid fossa. Pathologic glenoid version and inclination are then measured 3-dimensionally *(3D)* from the scapular and glenoid planes. The medial-lateral joint line position is measured as the distance between the glenoid center point and the scapular trigonum. The glenoid vault model *(inset)* is virtually placed into the glenoid of each preoperative computed tomography scan as a tool to define premorbid glenoid anatomy. Premorbid glenoid version and inclination are measured 3-dimensionally from the scapular plane and the plane of the glenoid vault surface. The premorbid medial-lateral joint line position is measured as the distance between the glenoid vault center point and the scapula trigonum. (**B-G**) Representative 2-dimensional orthogonal views relative to the scapular plane are used to confirm vault model position and demonstrate premorbid (**B-D**) and pathologic (**E-G**) version, inclination, and medial-lateral joint line position relative to each other.

as they required minor or no correction of the measured pathology. The frequency of cases corrected to different levels was compared between select groups using the Fisher exact test.

For type B2 and B3 glenoids, multivariate models were built to identify factors associated with better correction of version and the ML joint line relative to premorbid version and the premorbid joint line, respectively. The following factors were included in each model: (1) Walch type (B2 or B3), (2) glenoid component type (SG or AG), (3) preoperative ML joint line position relative to vault model, and (4) preoperative version relative to vault model. No strong collinearity was found among the included factors. Univariate comparisons were made in SAS software (version 9.4; SAS Institute, Cary, NC). Multivariate models were built using R software (version 3.4; R Foundation for Statistical Computing, Vienna, Austria). All tests were 2-sided with a significance level of .01 for univariate analyses to control for multiple comparisons and a significance level of .05 for the multivariate models.

Results

Summary statistics of preoperative pathologic measurements (CT1) and postoperative glenoid implant position (CT2) based on the modified Walch classification and implant type (SG or AG component) are shown in Table I. Mean preoperative-to-postoperative changes relative to pathologic (CT2 – CT1) and premorbid (CT2 – Vault) glenoid anatomy and mean postoperative humeral head

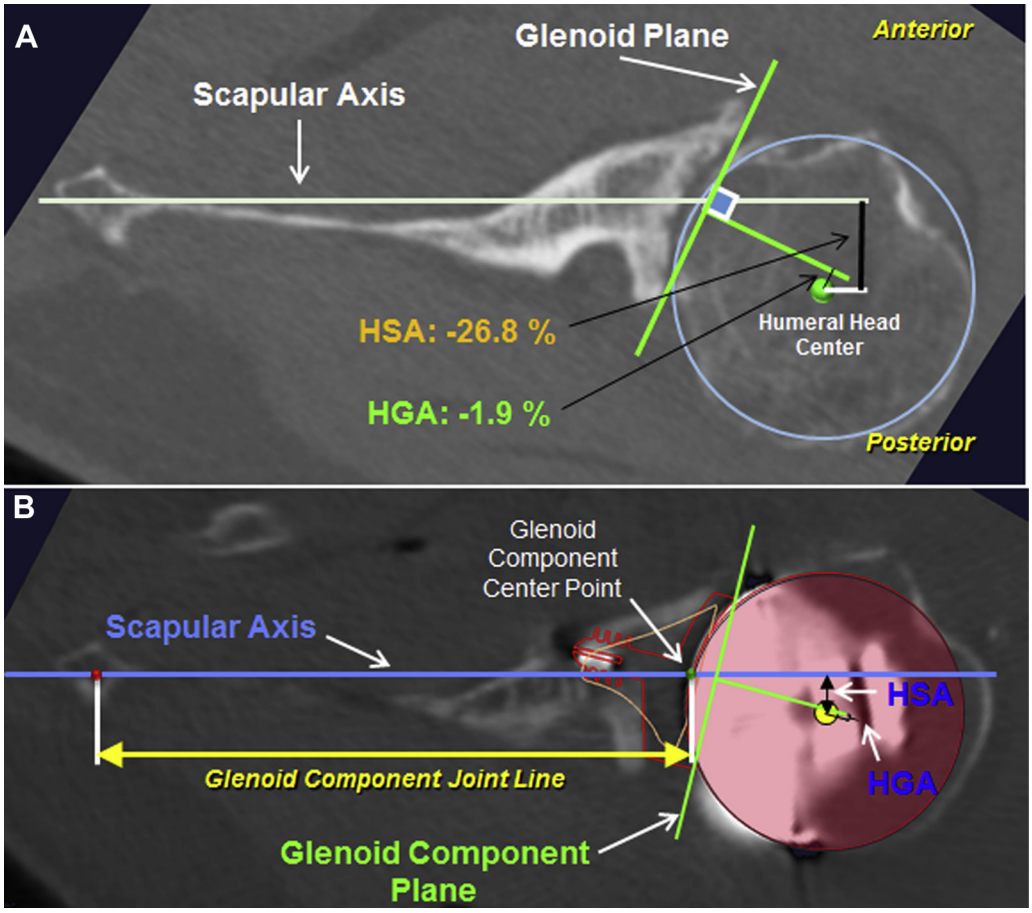

Figure 2 (**A**) Preoperative humeral head alignment is measured in the axial plane (anteroposterior) with respect to the scapular coordinate system, at the level of the glenoid center point. Best-fit sphere placement to the native humeral head is performed using a validated method to define the center of the humeral head, which is used for measurement of humeral scapular alignment (*HSA-AP*) and humeral glenoid alignment (*HGA-AP*). HSA-AP is the perpendicular distance from the humeral head center to the scapular axis. HGA-AP is the perpendicular distance from the humeral head center to a perpendicular line through the glenoid center point. Both HSA-AP and HGA-AP are expressed as a percentage of humeral head diameter. (**B**) Postoperative HSA-AP and HGA-AP are defined similarly to the preoperative measurements, but they reference the center of the humeral head component and center of the glenoid component. Both HSA-AP and HGA-AP are expressed as a percentage of humeral head diameter. The glenoid component medial-lateral joint line measurement is also shown, with the medial-lateral joint line position measured as the distance between the glenoid component center point and the scapula trigonum.

alignment (CT2) of the cohort with select group comparisons are shown in Table II. A summary of the relevant findings is highlighted later. No significant differences were seen in glenoid inclination changes across any of the compared groups.

Type A1 vs. type A2 glenoids with SG components

On average, correction to premorbid glenoid anatomy was significantly less in type A2 glenoids than in type A1 glenoids for the ML joint line position (–2.3 ± 2.1 mm vs. 1.1 ± 0.9 mm, $P < .001$) (Table II). Whereas 98% and 100% of type A1 glenoids were corrected to ≥–1 mm and ≥–3 mm of the premorbid ML joint line position, respectively, only 22% ($P < .001$) and 72% ($P < .001$) of type A2 glenoids, respectively, were corrected to these levels (Table III).

Type B2 glenoids with SG and AG components

On average, type B2 glenoids were significantly better corrected relative to pathologic glenoid anatomy using AG components compared with SG components in version (9.5° ± 6.4° vs. 2.5° ± 4.6°, $P < .001$) and the ML joint line position (2.5 ± 1.2 mm vs. 1.4 ± 1.3 mm, $P = .002$) (Table II). However, correction to premorbid version (–1.7° ± 6.6° vs. –3.9° ± 4.6°, $P = .19$) and correction to the premorbid ML joint line position (0.3 ± 1.6 mm vs. –0.4 ± 1.3 mm, $P = .085$) were not different between components, nor was postoperative HGA-AP (–1.4% ± 3.8% vs. –0.8% ± 3.8%, $P = .49$) (Table II).

Correction to premorbid version was not different between type B2 glenoids with AG components and type A1 glenoids with SG components (–1.7° ± 6.6° vs. –1.0° ±

Table I Preoperative and postoperative measurements of glenoid anatomy and preoperative humeral head alignment in cases with type A1, A2, B2, or B3 glenoids

Factor	Mean ± SD within group						
	Total (N = 154)	A1 SG (n = 48)	A2 SG (n = 18)	B2 SG (n = 22)	B2 AG (n = 31)	B3 SG (n = 12)	B3 AG (n = 23)
Glenoid version, °							
CT1	−13.1 ± 8.4	−5.7 ± 4.2	−6.6 ± 4.9	−13.7 ± 5.5	−20.2 ± 5.9	−16.3 ± 3.2	−22.3 ± 5.8
Vault	−6.5 ± 3.6	−5.0 ± 2.4	−3.3 ± 3.8	−7.2 ± 2.4	−9.0 ± 3.1	−5.7 ± 3.5	−8.4 ± 3.7
CT2	−8.7 ± 5.9	−6.1 ± 5.2	−7.1 ± 5.2	−11.1 ± 5.5	−10.7 ± 6.5	−11.7 ± 4.8	−9.0 ± 5.4
Glenoid inclination, °							
CT1	4.7 ± 4.9	5.0 ± 4.5	4.4 ± 4.9	3.8 ± 4.8	6.0 ± 5.4	3.0 ± 3.7	4.2 ± 5.4
Vault	5.8 ± 3.9	5.8 ± 3.6	4.0 ± 4.5	5.5 ± 4.5	7.2 ± 4.0	5.7 ± 3.1	5.7 ± 3.3
CT2	5.9 ± 5.1	6.5 ± 4.2	5.7 ± 6.8	4.9 ± 6.6	6.6 ± 5.5	5.2 ± 3.7	5.5 ± 4.2
Glenoid ML joint line position (CT1 – Vault), mm	−2.9 ± 2.1	−1.5 ± 0.75	−4.9 ± 0.9	−1.8 ± 0.72	−2.2 ± 1.4	−4.3 ± 2.1	−5.4 ± 2.1
HSA-AP on CT1, %	−15.5 ± 11.1	−6.6 ± 7.2	−6.6 ± 7.2	−19.6 ± 6.7	−26.9 ± 10.2	−17.2 ± 3.4	−21.1 ± 6.7
HGA-AP on CT1, %	−4.2 ± 6.8	−1.4 ± 4.9	−1.1 ± 4.7	−8.0 ± 5.1	−9.6 ± 9.0	−3.3 ± 4.4	−1.7 ± 4.8

SD, standard deviation; *SG*, standard glenoid component; *AG*, augmented glenoid component; *CT1*, preoperative computed tomography scan; *Vault*, premorbid anatomy estimated from vault model; *CT2*, postoperative computed tomography scan within 3 months of surgery; *ML*, medial-lateral; *HSA*, humeral scapular alignment; *AP*, anteroposterior; *HGA*, humeral glenoid alignment.
Data are presented as mean ± SD for the groups based on the modified Walch classification and glenoid component type. Preoperative joint line medialization was defined as the difference between the pathologic ML joint line position and the premorbid ML joint line position (CT1 – Vault).

4.0°, $P = .57$) (Table II). Although correction relative to the premorbid ML joint line position was significantly less in type B2 glenoids with AG components than in type A1 glenoids with SG components (0.3 ± 1.6 mm vs. 1.1 ± 0.9 mm, $P = .006$), the premorbid ML joint line position was restored on average in both groups (Table II, Fig. 3). Postoperative HGA-AP was not different between groups (–1.4% ± 3.8% vs. –0.2% ± 3.7%, $P = .17$) (Table II).

Type B3 glenoids with SG and AG components

On average, type B3 glenoids were significantly better corrected relative to pathologic glenoid anatomy using AG components compared with SG components in version (13.2° ± 7.1° vs. 4.6° ± 4.8°, $P < .001$) and the difference was nearly significant for the ML joint line position (3.2 ± 1.4 mm vs. 2.2 ± 0.7 mm, $P = .017$) (Table II). Correction to premorbid version was also significantly better for AG components compared with SG components (–0.6° ± 5.1° vs. –6.1° ± 6.1°, $P = .009$). However, correction relative to the premorbid ML joint line position was not different between components (–2.2 ± 2.1 mm vs. –2.1 ± 1.6 mm, $P = .92$), nor was postoperative HGA-AP (–0.5% ± 3.0% vs. 1.6% ± 4.2%, $P = .088$) (Table II).

Correction to premorbid version was not different between type B3 glenoids with AG components and type A1 glenoids with SG components (–0.6° ± 5.1° vs. –1.0° ± 4.0°, $P = .72$) (Table II). However, correction relative to the premorbid ML joint line position was significantly less in type B3 glenoids with AG components than in type A1 glenoids with SG components (–2.2 ± 2.1 mm vs. 1.1 ± 0.9 mm, $P < .001$) (Table II, Fig. 3). Postoperative HGA-AP was not different between groups (–0.5% ± 3.0% vs. –0.2% ± 3.7%, $P = .77$) (Table II).

Type B2 vs. type B3 glenoids

On average, correction to premorbid version was not different between type B3 and B2 glenoids with AG components (–0.6° ± 5.1° vs. –1.7° ± 6.6°, $P = .52$) (Table II). ML joint line correction relative to pathologic anatomy was also not significantly different between type B3 and B2 glenoids with AG components (3.2 ± 1.4 mm vs. 2.5 ± 1.2 mm, $P = .042$); however, correction relative to the premorbid ML joint line position was significantly less in type B3 glenoids than in type B2 glenoids with AG components (–2.2 ± 2.1 mm vs. 0.3 ± 1.6 mm, $P < .001$) (Table II). Postoperative HGA-AP was not different between groups (–0.5% ± 3.0% vs. –1.4% ± 3.8%, $P = .33$) (Table II).

Surgical correction relative to premorbid version and the premorbid ML joint line position in individual type B2 and B3 cases treated with SG and AG components are graphically depicted in Figures 4 and 5, respectively. The results showed that 86% of type B2 glenoids with SG components and 87% of type B2 glenoids with AG components were corrected to within 10° of premorbid version and 3 mm of the premorbid ML joint line position whereas 58% ($P = .10$) of type B3 glenoids with SG components and 70% ($P = .17$) of type B3 glenoids with AG components were corrected to these levels (Table IV).

On multivariate modeling of factors associated with better postoperative correction of type B2 and B3 glenoid

Table II Preoperative-to-postoperative changes relative to pathologic (CT2 – CT1) and premorbid (CT2 – Vault) glenoid anatomy and postoperative humeral head alignment (CT2) in cases with type A1, A2, B2, or B3 glenoids

Factor	Mean ± SD within group							Statistical analysis between groups					
	Total (N = 154)	A1 SG (n = 48)	A2 SG (n = 18)	B2 SG (n = 22)	B2 AG (n = 31)	B3 SG (n = 12)	B3 AG (n = 23)	A2 SG vs. A1 SG	B2 AG vs. B2 SG	B2 AG vs. A1 SG	B3 AG vs. B3 SG	B3 AG vs. A1 SG	B3 AG vs. B2 AG
Glenoid version, °													
CT2 – CT1	−0.4 ± 3.6	−0.4 ± 3.6	−0.5 ± 3.9	2.5 ± 4.6	9.5 ± 6.4	4.6 ± 4.8	13.2 ± 7.1	.92	<.001*	<.001*	<.001*	<.001*	.046
CT2 – Vault	−1.8 ± 4.0	−1.0 ± 4.0	−3.8 ± 3.5	−3.9 ± 4.6	−1.7 ± 6.6	−6.1 ± 6.1	−0.6 ± 5.1	.012	.19	.57	.009*	.72	.52
Glenoid inclination, °													
CT2 – CT1	1.5 ± 4.0	1.6 ± 4.1	1.3 ± 3.8	1.0 ± 5.4	0.6 ± 4.6	2.2 ± 4.7	1.3 ± 5.1	.82	.74	.32	.61	.79	.60
CT2 – Vault	1.0 ± 4.7	0.7 ± 4.7	1.7 ± 4.8	−0.7 ± 5.6	−0.6 ± 4.7	−0.5 ± 5.6	−0.3 ± 4.2	.47	.94	.24	.90	.40	.79
Glenoid ML joint line position, mm													
CT2 – CT1	2.6 ± 0.7	2.6 ± 0.6	2.6 ± 0.9	1.4 ± 1.3	2.5 ± 1.2	2.2 ± 0.7	3.2 ± 1.4	.94	.002*	.54	.017	.012	.042
CT2 – Vault	0.2 ± 2.0	1.1 ± 0.9	−2.3 ± 2.1	−0.4 ± 1.3	0.3 ± 1.6	−2.1 ± 1.6	−2.2 ± 2.1	<.001*	.085	.006*	.92	<.001*	<.001*
HSA-AP on CT2, %	−6.3 ± 7.0	−6.0 ± 6.9	−6.9 ± 7.3	−14.7 ± 5.8	−17.2 ± 9.3	−11.0 ± 5.8	−12.3 ± 7.6	.64	.26	<.001*	.61	<.001*	.042
HGA-AP on CT2, %	−0.5 ± 3.9	−0.2 ± 3.7	−1.0 ± 4.4	−0.8 ± 2.8	−1.4 ± 3.8	1.6 ± 4.2	−0.50 ± 3.0	.49	.49	.17	.088	.77	.33

CT2, postoperative computed tomography scan within 3 months of surgery; *CT1*, preoperative computed tomography scan; *Vault*, premorbid anatomy estimated from vault model; *SD*, standard deviation; *SG*, standard glenoid component; *AG*, augmented glenoid component; *ML*, medial-lateral; *HSA*, humeral scapular alignment; *AP*, anteroposterior; *HGA*, humeral glenoid alignment.

Data are presented as mean ± SD for the groups based on the modified Walch classification and glenoid component type. *P* values are presented for select group comparisons of these preoperative-to-postoperative changes using 2-sample *t* tests between groups. A significance level of .01 was used to control for multiple comparisons.

* Statistically significant.

Table III Frequencies of cases with type A1 or A2 glenoids treated with SG components reaching 3 levels of glenoid ML joint line correction relative to premorbid ML joint line position, as estimated from vault model

	Total (N = 66), n (%)	A1 SG (n = 48), n (%)	A2 SG (n = 18), n (%)	*P* value
Correction level (CT2 – Vault) ≥ −1 mm of ML joint line	51 of 66 (77)	47 of 48 (98)	4 of 18 (22)	<.001*
Correction level (CT2 – Vault) ≥ −3 mm of ML joint line	61 of 66 (92)	48 of 48 (100)	13 of 18 (72)	<.001*
Correction level (CT2 – Vault) ≥ −5 mm of ML joint line	64 of 66 (97)	48 of 48 (100)	16 of 18 (89)	.071

SG, standard glenoid; *ML*, medial-lateral; *Vault*, premorbid anatomy estimated from vault model.
P values are presented for group comparisons at the 3 levels of joint line correction performed using the Fisher exact test.
* Statistically significant.

pathology, an AG component ($P < .001$) and better preoperative version relative to the vault model ($P < .001$) were significantly associated with better version correction to premorbid version. Similarly, an AG component ($P = .002$) and a better preoperative ML joint line position relative to the vault model ($P < .001$) were significantly associated with better ML joint line correction to the premorbid joint line.

Discussion

The purpose of this study was to quantify correction of glenoid deformity and humeral head alignment as a function of preoperative pathology (modified Walch classification) and glenoid implant type using 3D CT analysis. We assessed correction relative to both pathologic and premorbid anatomy. As hypothesized, we found that there are limits to surgical corrections with current implants based on the modified Walch classification and the severity of preoperative pathologic measurements, particularly glenoid version and the ML joint line position. The postoperative glenoid component ML joint line position in type A1 and A2 glenoids with SG components was associated with the severity of preoperative glenoid joint line medialization, with average correction to the premorbid ML joint line significantly less for type A2 glenoids. In type B2 and B3 glenoids, a posteriorly stepped AG component corrected preoperative glenoid version better than an SG component, with the AG component and less severe preoperative retroversion significantly associated with better postoperative version correction relative to the vault model on multivariate modeling. However, the preoperative ML joint line position was not a significant factor in this model. Similarly, an AG component and less severe preoperative joint line medialization were significantly associated with better postoperative ML joint line correction relative to the vault model on multivariate modeling. Preoperative version was not a significant factor in this model.

In contrast, we found no significant differences in group comparisons for other quantitative measurements postoperatively, such as glenoid inclination and humeral head alignment relative to the glenoid axis (HGA-AP). In particular, postoperative (CT2) HGA-AP was not significantly different across all of the group comparisons, demonstrating that a well-centered humeral head can be achieved with currently available implants, even in the setting of more advanced posterior glenoid bone loss with posterior subluxation of the humeral head (type B2 and B3 glenoids). Although humeral head alignment relative to the scapular axis (HSA-AP) did show differences postoperatively in some group comparisons (type B2 or B3 glenoids with AG components vs. type A1 glenoids with SG components), HSA-AP has previously been shown to be strongly associated with glenoid version[41] and these findings were likely a result of differences in glenoid component version between the groups, as the HGA-AP results demonstrated that the humeral head was well centered across all groups.

The goal of surgical correction in our study was to select the glenoid component position and type (SG or AG component), using 3D preoperative surgical planning, that best restored premorbid anatomy as defined by the glenoid vault model. Although recommendations on surgical correction in anatomic TSA vary in the literature, the ability to accurately assess postoperative implant position regardless of the surgical goals is essential to determine which factors related to implant position and surgical correction most impact clinical outcomes over time. Currently, there are no definitive guidelines for surgical correction that have been shown to result in a clinically significant difference in outcomes, with minimal available data in clinical cohorts accurately assessing pathologic correction and implant position following anatomic TSA. Although correction relative to preoperative pathology is important to assess, we also believe it is essential to determine corrections relative to the premorbid state to better understand the importance of restoration of premorbid anatomy to clinical outcomes. The use of the glenoid vault model, a standardized 3D model shown to be predictive of premorbid anatomy in a pathologic glenoid,[7,12,21,35,44] allowed us to make such assessments. In particular, we found that correction of glenoid

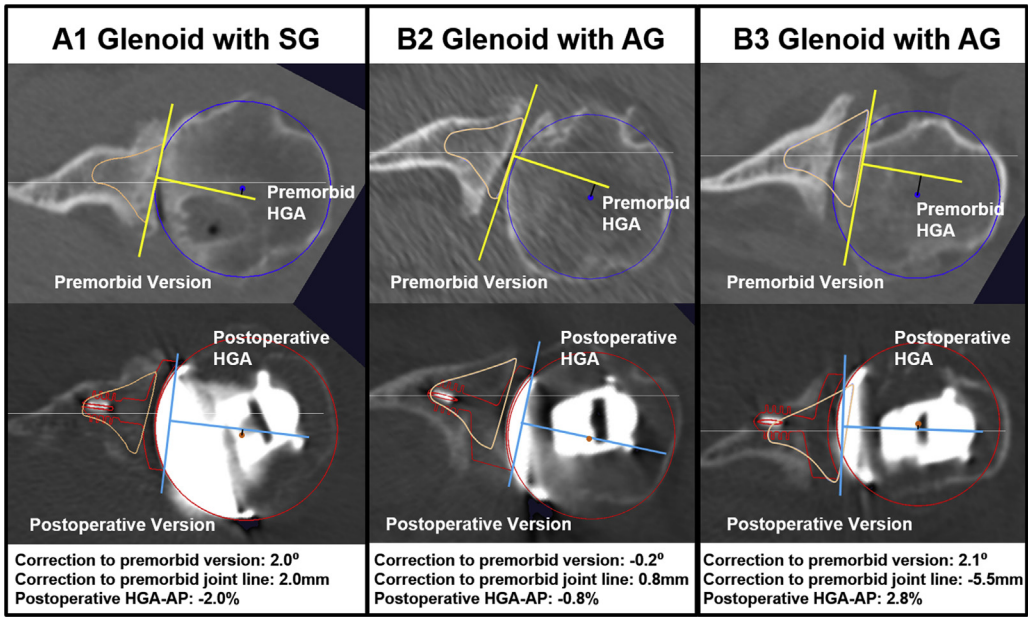

Figure 3 Comparison of type A1 glenoid treated with standard glenoid *(SG)* component, type B2 glenoid treated with posteriorly augmented glenoid *(AG)* component, and type B3 glenoid treated with AG component. The *top row* shows preoperative computed tomography scans with the glenoid vault model (*pink outline*) placed into the pathologic glenoid. Premorbid version, the premorbid medial-lateral joint line position, and premorbid humeral glenoid alignment (*HGA-AP*) are shown. The *bottom row* shows postoperative computed tomography scans with the position of the glenoid and humeral head components outlined in *red*. Glenoid component version, the medial-lateral joint line position, and HGA-AP are shown. The vault model remains in the same position on the postoperative computed tomography scans to measure preoperative-to-postoperative changes relative to premorbid anatomy. All 3 cases show good version correction relative to premorbid version, with a centered humeral head (HGA-AP) postoperatively. However, whereas the type A1 glenoid with an SG component and the type B2 glenoid with an AG component show restoration of the premorbid medial-lateral joint line position, the joint line of the type B3 glenoid with an AG component remains persistently medialized postoperatively (–5.5 mm relative to the premorbid joint line position).

pathology back to premorbid version and the premorbid ML joint line position can be accomplished in type B2 glenoids and, to a lesser extent, type B3 glenoids with a posteriorly stepped AG component and is comparable to use of an SG component in type A1 glenoids.

Prior studies have demonstrated that correction of more advanced glenoid retroversion, posterior humeral head subluxation, and joint line medialization due to posterior glenoid bone loss may not always be possible in anatomic TSA with routine surgical techniques.[6,13,20,32] Our study further defines the limitations on pathologic corrections based on both the modified Walch classification and implant type using precise 3D CT measurements in a large clinical cohort. Restoration of the premorbid ML joint line position may not always be possible with SG components or posteriorly stepped AG components in cases with more advanced glenoid bone loss, particularly when significant central bone loss develops, as is commonly seen in type A2 (central wear) and type B3 (central and posterior wear) glenoids. In this study, the premorbid ML joint line position was restored on average with AG components in type B2 glenoids, which show more posterior than central wear. This also likely occurs a result of the shape of the posteriorly stepped AG component closely matching the shape of the type B2 deformity. In contrast, the average ML joint line position remained medialized relative to the premorbid joint line in type A2 glenoids with SG components, type B3 glenoids with SG components, and type B3 glenoids with posteriorly stepped AG components. Only 72% of type A2 glenoids were corrected to $\geq$–3 mm of the premorbid ML joint line position. Similarly, only 58% of type B3 glenoids with SG components and 70% of type B3 glenoids with AG components were corrected to within 10° of premorbid version and 3 mm of the premorbid ML joint line position, with the majority of the outliers due to joint line medialization >3 mm. These analyses potentially suggest that the availability of 3-mm-thicker glenoid components would allow for better restoration of the premorbid ML joint line position in cases with more advanced central glenoid bone loss (types A2 and B3). A wedge-shaped AG component may also better match the bony deformity of the type B3 glenoid, as the posteriorly stepped AG component does not fit this deformity as well as a type B2 defect. ML joint line restoration likely has long-term clinical consequences, as we have previously shown that more preoperative joint line medialization is present in patients with AG components that develop central peg osteolysis on plain radiographs at minimum 2-year follow-up.[15]

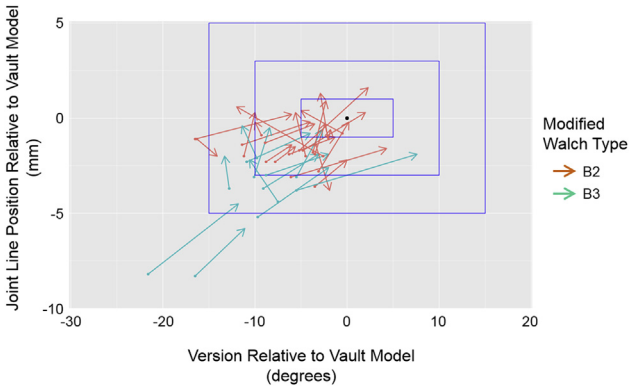

Figure 4 Surgical correction relative to premorbid version and medial-lateral (ML) joint line position of type B2 and B3 cases treated with standard glenoid components. The axes represent glenoid version and the ML joint line position relative to the vault model. Each *arrow* signifies a surgical case, with its starting point *(dot)* representing glenoid version and the ML joint line position preoperatively and its endpoint (*arrowhead*) representing glenoid component version and the ML joint line position postoperatively. Threshold levels are marked as *boxes* around 0° of premorbid version and 0 mm of the premorbid ML joint line (*black circle*) with the following cutoffs: (1) 5° of premorbid version and 1 mm of the premorbid ML joint line, (2) 10° of premorbid version and 3 mm of the premorbid ML joint line, and (3) 15° of premorbid version and 5 of the mm premorbid ML joint line.

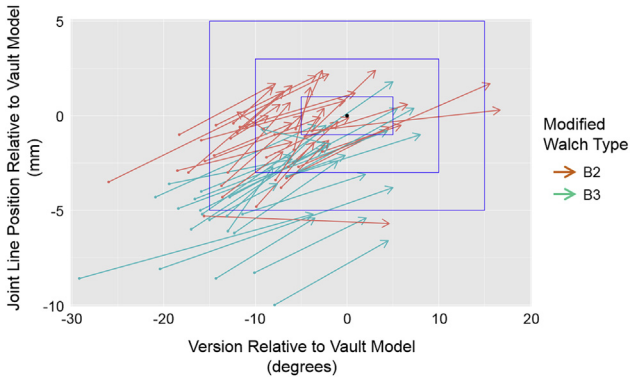

Figure 5 Surgical correction relative to premorbid version and medial-lateral (ML) joint line position of type B2 and B3 cases treated with posteriorly augmented glenoid components. The axes represent glenoid version and the ML joint line position relative to the vault model. Each *arrow* signifies a surgical case, with its starting point (*dot*) representing glenoid version and the ML joint line position preoperatively and its endpoint (*arrowhead*) representing glenoid component version and the ML joint line position postoperatively. Threshold levels are marked as *boxes* around 0° of premorbid version and a 0-mm premorbid ML joint line (*black circle*) with the following cutoffs: (1) 5° of premorbid version and 1 mm of the premorbid ML joint line, (2) 10° of premorbid version and 3 mm of the premorbid ML joint line, and (3) 15° of premorbid version and 5 mm of the premorbid ML joint line.

There are limitations to this study. First, as humeral head alignment (HSA-AP and HGA-AP) was assessed prior to full shoulder rehabilitation, these measurements could change as the rotator cuff and deltoid, as well as other periscapular muscles, strengthen over time. Second, although large for the study design, the current cohort still represents a relatively small sample for robust statistical analysis. Third, we report on only immediate postoperative implant position. The clinical consequences of these surgical corrections are still unknown. For example, although statistically significant, the absolute differences in the ML joint line position between the modified Walch classification and implant types were, at times, small, and the clinical significance is not yet known. We plan to use our methods of 3D CT analysis for continued clinical and imaging follow-up of the current cohort to better understand

Table IV Frequencies of cases with type B2 or B3 glenoids treated with SG or AG component reaching 3 levels of glenoid version and ML joint line correction relative to premorbid version and ML joint line position, as estimated from vault model

	Total (N = 88), n (%)	SG			AG		
		B2 (n = 22), n (%)	B3 (n = 12), n (%)	*P* value	B2 (n = 31), n (%)	B3 (n = 23), n (%)	*P* value
Correction level (CT2 – Vault) within 5° of version and 1 mm of ML joint line	21 of 88 (24)	9 of 22 (41)	2 of 12 (17)	.25	7 of 31 (23)	3 of 23 (13)	.49
Correction level (CT2 – Vault) within 10° of version and 3 mm of ML joint line	69 of 88 (78)	19 of 22 (86)	7 of 12 (58)	.10	27 of 31 (87)	16 of 23 (70)	.17
Correction level (CT2 – Vault) within 15° of version and 5 mm of ML joint line	80 of 88 (91)	22 of 22 (100)	11 of 12 (92)	.35	28 of 31 (90)	19 of 23 (83)	.44

SG, standard glenoid; *AG*, augmented glenoid; *ML*, medial-lateral; *Vault*, premorbid anatomy estimated from vault model.
P values are presented for group comparisons at the 3 levels of version and joint line correction performed using the Fisher exact test.

whether such differences are clinically relevant, and if so, future work will be needed to determine the ability to consistently make pathologic corrections at the time of surgery with available implants in larger clinical cohorts involving more surgeons.

This study has notable strengths. The results demonstrate the ability of experienced shoulder surgeons to place a glenoid implant during surgery to achieve planned corrections. All patients underwent 3D CT preoperative surgical planning with a consistent set of rules for component placement, which our group has shown results in more accurate glenoid component placement and selection when compared with the use of standard 2-dimensional preoperative CT without planning and PSI.[14,24,25] The unique 3D CT imaging analysis also has not been possible with standard radiographs or CT scans, which lack precision and accuracy to determine preoperative-to-postoperative changes and measure postoperative changes over time.[2-4,17,28,33,37,52] Further follow-up with these methods will provide the ability to determine the long-term clinical consequences of the current findings, including whether more closely restoring premorbid anatomy is associated with better clinical outcomes and implant longevity.

Conclusion

In cases with posterior glenoid bone loss and retroversion (type B2 or B3 glenoids), an AG component can better correct retroversion and the glenoid ML joint line position compared with an SG component. Correction back to premorbid version is possible in type B2 and B3 glenoids with an AG component and is comparable to use of an SG component in type A1 glenoids. However, there are limits to pathologic corrections with current implants. Specifically, restoration of the premorbid ML joint line position may not always be possible with SG or AG components in cases with more advanced central glenoid bone loss (type A2 or B3 glenoids). Further follow-up is needed to determine the long-term clinical impact of these findings.

Acknowledgments

The authors acknowledge Catherine Shemo, BS, for her assistance with institutional review board approval and research compliance.

Disclaimer

The State of Ohio Technology Development Fund (TIOSO) provided funding for this study.

Joseph P. Iannotti receives royalty income from DePuy Synthes. All the other authors, their immediate families, and any research foundations with which they are affiliated have not received any financial payments or other benefits from any commercial entity related to the subject of this article.

References

1. Bercik MJ, Kruse K II, Yalizis M, Gauci MO, Chaoui J, Walch G. A modification to the Walch classification of the glenoid in primary glenohumeral osteoarthritis using three-dimensional imaging. J Shoulder Elbow Surg 2016;25:1601-6. https://doi.org/10.1016/j.jse.2016.03.010
2. Bryce CD, Davison AC, Lewis GS, Wang L, Flemming DJ, Armstrong AD. Two-dimensional glenoid version measurements vary with coronal and sagittal scapular rotation. J Bone Joint Surg Am 2010;92:692-9. https://doi.org/10.2106/JBJS.I.00177
3. Bryce CD, Pennypacker JL, Kulkarni N, Paul EM, Hollenbeak CS, Mosher TJ, et al. Validation of three-dimensional models of in situ scapulae. J Shoulder Elbow Surg 2008;17:825-32. https://doi.org/10.1016/j.jse.2008.01.141
4. Budge MD, Lewis GS, Schaefer E, Coquia S, Flemming DJ, Armstrong AD. Comparison of standard two-dimensional and three-dimensional corrected glenoid version measurements. J Shoulder Elbow Surg 2011;20:577-83. https://doi.org/10.1016/j.jse.2010.11.003
5. Chan K, Knowles NK, Chaoui J, Gauci MO, Ferreira LM, Walch G, et al. Characterization of the Walch B3 glenoid in primary osteoarthritis. J Shoulder Elbow Surg 2017;26:909-14. https://doi.org/10.1016/j.jse.2016.10.003
6. Clavert P, Millett PJ, Warner JJ. Glenoid resurfacing: what are the limits to asymmetric reaming for posterior erosion? J Shoulder Elbow Surg 2007;16:843-8. https://doi.org/10.1016/j.jse.2007.03.015
7. Codsi MJ, Bennetts C, Gordiev K, Boeck DM, Kwon Y, Brems J, et al. Normal glenoid vault anatomy and validation of a novel glenoid implant shape. J Shoulder Elbow Surg 2008;17:471-8. https://doi.org/10.1016/j.jse.2007.08.010
8. Denard PJ, Walch G. Current concepts in the surgical management of primary glenohumeral arthritis with a biconcave glenoid. J Shoulder Elbow Surg 2013;22:1589-98. https://doi.org/10.1016/j.jse.2013.06.017
9. Donohue KW, Ricchetti ET, Ho JC, Iannotti JP. The association between rotator cuff muscle fatty infiltration and glenoid morphology in glenohumeral osteoarthritis. J Bone Joint Surg Am 2018;100:381-7. https://doi.org/10.2106/JBJS.17.00232
10. Farron A, Terrier A, Buchler P. Risks of loosening of a prosthetic glenoid implanted in retroversion. J Shoulder Elbow Surg 2006;15:521-6. https://doi.org/10.1016/j.jse.2005.10.003
11. Favorito PJ, Freed RJ, Passanise AM, Brown MJ. Total shoulder arthroplasty for glenohumeral arthritis associated with posterior glenoid bone loss: results of an all-polyethylene, posteriorly augmented glenoid component. J Shoulder Elbow Surg 2016;25:1681-9. https://doi.org/10.1016/j.jse.2016.02.020
12. Ganapathi A, McCarron JA, Chen X, Iannotti JP. Predicting normal glenoid version from the pathologic scapula: a comparison of 4 methods in 2- and 3-dimensional models. J Shoulder Elbow Surg 2011;20:234-44. https://doi.org/10.1016/j.jse.2010.05.024
13. Gillespie R, Lyons R, Lazarus M. Eccentric reaming in total shoulder arthroplasty: a cadaveric study. Orthopedics 2009;32:21. https://doi.org/10.3928/01477447-20090101-07
14. Hendel MD, Bryan JA, Barsoum WK, Rodriguez EJ, Brems JJ, Evans PJ, et al. Comparison of patient-specific instruments with standard surgical instruments in determining glenoid component

position: a randomized prospective clinical trial. J Bone Joint Surg Am 2012;94:2167-75. https://doi.org/10.2106/JBJS.K.01209
15. Ho JC, Amini MH, Entezari V, Jun BJ, Alolabi B, Ricchetti ET, et al. Clinical and radiographic outcomes of a posteriorly augmented glenoid component in anatomic total shoulder arthroplasty for primary osteoarthritis with posterior glenoid bone loss. J Bone Joint Surg Am 2018;100:1934-48. https://doi.org/10.2106/JBJS.17.01282
16. Ho JC, Sabesan VJ, Iannotti JP. Glenoid component retroversion is associated with osteolysis. J Bone Joint Surg Am 2013;95:e82. https://doi.org/10.2106/JBJS.L.00336
17. Ho JC, Youderian A, Davidson IU, Bryan J, Iannotti JP. Accuracy and reliability of postoperative radiographic measurements of glenoid anatomy and relationships in patients with total shoulder arthroplasty. J Shoulder Elbow Surg 2013;22:1068-77. https://doi.org/10.1016/j.jse.2012.11.015
18. Hopkins AR, Hansen UN, Amis AA, Emery R. The effects of glenoid component alignment variations on cement mantle stresses in total shoulder arthroplasty. J Shoulder Elbow Surg 2004;13:668-75. https://doi.org/10.1016/s1058274604001399
19. Iannotti J, Baker J, Rodriguez E, Brems J, Ricchetti E, Mesiha M, et al. Three-dimensional preoperative planning software and a novel information transfer technology improve glenoid component positioning. J Bone Joint Surg Am 2014;96:e71. https://doi.org/10.2106/JBJS.L.01346
20. Iannotti JP, Greeson C, Downing D, Sabesan V, Bryan JA. Effect of glenoid deformity on glenoid component placement in primary shoulder arthroplasty. J Shoulder Elbow Surg 2012;21:48-55. https://doi.org/10.1016/j.jse.2011.02.011
21. Iannotti JP, Jun BJ, Patterson TE, Ricchetti ET. Quantitative measurement of osseous pathology in advanced glenohumeral osteoarthritis. J Bone Joint Surg Am 2017;99:1460-8. https://doi.org/10.2106/JBJS.16.00869
22. Iannotti JP, Lappin KE, Klotz CL, Reber EW, Swope SW. Liftoff resistance of augmented glenoid components during cyclic fatigue loading in the posterior-superior direction. J Shoulder Elbow Surg 2013;22:1530-6. https://doi.org/10.1016/j.jse.2013.01.018
23. Iannotti JP, Ricchetti ET, Rodriguez EJ, Bryan JA. Development and validation of a new method of 3-dimensional assessment of glenoid and humeral component position after total shoulder arthroplasty. J Shoulder Elbow Surg 2013;22:1413-22. https://doi.org/10.1016/j.jse.2013.01.005
24. Iannotti JP, Walker K, Rodriguez E, Patterson TE, Jun BJ, Ricchetti ET. Accuracy of 3-dimensional planning, implant templating, and patient-specific instrumentation in anatomic total shoulder arthroplasty. J Bone Joint Surg Am 2019;101:446-57. https://doi.org/10.2106/JBJS.17.01614
25. Iannotti JP, Weiner S, Rodriguez E, Subhas N, Patterson TE, Jun BJ, et al. Three-dimensional imaging and templating improve glenoid implant positioning. J Bone Joint Surg Am 2015;97:651-8. https://doi.org/10.2106/JBJS.N.00493
26. Klika BJ, Wooten CW, Sperling JW, Steinmann SP, Schleck CD, Harmsen WS, et al. Structural bone grafting for glenoid deficiency in primary total shoulder arthroplasty. J Shoulder Elbow Surg 2014;23:1066-72. https://doi.org/10.1016/j.jse.2013.09.017
27. Kwon YW, Powell KA, Yum JK, Brems JJ, Iannotti JP. Use of three-dimensional computed tomography for the analysis of the glenoid anatomy. J Shoulder Elbow Surg 2005;14:85-90. https://doi.org/10.1016/j.jse.2004.04.011
28. Lazarus MD, Jensen KL, Southworth C, Matsen FA III. The radiographic evaluation of keeled and pegged glenoid component insertion. J Bone Joint Surg Am 2002;84-A:1174-82.
29. Mizuno N, Denard PJ, Raiss P, Walch G. Reverse total shoulder arthroplasty for primary glenohumeral osteoarthritis in patients with a biconcave glenoid. J Bone Joint Surg Am 2013;95:1297-304. https://doi.org/10.2106/JBJS.L.00820
30. Morsbach F, Bickelhaupt S, Wanner GA, Krauss A, Schmidt B, Alkadhi H. Reduction of metal artifacts from hip prostheses on CT images of the pelvis: value of iterative reconstructions. Radiology 2013;268:237-44. https://doi.org/10.1148/radiol.13122089
31. Nelder JA, Mead R. A simplex method for function minimization. Comput J 1965;7:308-13.
32. Nowak DD, Bahu MJ, Gardner TR, Dyrszka MD, Levine WN, Bigliani LU, et al. Simulation of surgical glenoid resurfacing using three-dimensional computed tomography of the arthritic glenohumeral joint: the amount of glenoid retroversion that can be corrected. J Shoulder Elbow Surg 2009;18:680-8. https://doi.org/10.1016/j.jse.2009.03.019
33. Nyffeler RW, Jost B, Pfirrmann CW, Gerber C. Measurement of glenoid version: conventional radiographs versus computed tomography scans. J Shoulder Elbow Surg 2003;12:493-6. https://doi.org/10.1016/S1058274603001812
34. Pluim JP, Maintz JB, Viergever MA. Mutual-information-based registration of medical images: a survey. IEEE Trans Med Imaging 2003;22:986-1004. https://doi.org/10.1109/TMI.2003.815867
35. Ricchetti ET, Hendel MD, Collins DN, Iannotti JP. Is premorbid glenoid anatomy altered in patients with glenohumeral osteoarthritis? Clin Orthop Relat Res 2013;471:2932-9. https://doi.org/10.1007/s11999-013-3069-5
36. Ricchetti ET, Jun BJ, Cain RA, Youderian A, Rodriguez EJ, Kusin D, et al. Sequential 3-dimensional computed tomography analysis of implant position following total shoulder arthroplasty. J Shoulder Elbow Surg 2018;27:983-92. https://doi.org/10.1016/j.jse.2017.12.012
37. Rozing PM, Obermann WR. Osteometry of the glenohumeral joint. J Shoulder Elbow Surg 1999;8:438-42.
38. Sabesan V, Callanan M, Ho J, Iannotti JP. Clinical and radiographic outcomes of total shoulder arthroplasty with bone graft for osteoarthritis with severe glenoid bone loss. J Bone Joint Surg Am 2013;95:1290-6. https://doi.org/10.2106/JBJS.L.00097
39. Sabesan V, Callanan M, Sharma V. Guidelines for the selection of optimal glenoid augment size for moderate to severe glenohumeral osteoarthritis. J Shoulder Elbow Surg 2014;23:974-81. https://doi.org/10.1016/j.jse.2013.09.022
40. Sabesan V, Callanan M, Sharma V, Iannotti JP. Correction of acquired glenoid bone loss in osteoarthritis with a standard versus an augmented glenoid component. J Shoulder Elbow Surg 2014;23:964-73. https://doi.org/10.1016/j.jse.2013.09.019
41. Sabesan VJ, Callanan M, Youderian A, Iannotti JP. 3D CT assessment of the relationship between humeral head alignment and glenoid retroversion in glenohumeral osteoarthritis. J Bone Joint Surg Am 2014;96:e64. https://doi.org/10.2106/JBJS.L.00856
42. Scalise JJ, Bryan J, Polster J, Brems JJ, Iannotti JP. Quantitative analysis of glenoid bone loss in osteoarthritis using three-dimensional computed tomography scans. J Shoulder Elbow Surg 2008;17:328-35. https://doi.org/10.1016/j.jse.2007.07.013
43. Scalise JJ, Codsi MJ, Bryan J, Brems JJ, Iannotti JP. The influence of three-dimensional computed tomography images of the shoulder in preoperative planning for total shoulder arthroplasty. J Bone Joint Surg Am 2008;90:2438-45. https://doi.org/10.2106/JBJS.G.01341
44. Scalise JJ, Codsi MJ, Bryan J, Iannotti JP. The three-dimensional glenoid vault model can estimate normal glenoid version in osteoarthritis. J Shoulder Elbow Surg 2008;17:487-91. https://doi.org/10.1016/j.jse.2007.09.006
45. Stephens SP, Spencer EE, Wirth MA. Radiographic results of augmented all-polyethylene glenoids in the presence of posterior glenoid bone loss during total shoulder arthroplasty. J Shoulder Elbow Surg 2017;26:798-803. https://doi.org/10.1016/j.jse.2016.09.053
46. Subhas N, Primak AN, Obuchowski NA, Gupta A, Polster JM, Krauss A, et al. Iterative metal artifact reduction: evaluation and optimization of technique. Skeletal Radiol 2014;43:1729-35. https://doi.org/10.1007/s00256-014-1987-2

47. Terrier A, Buchler P, Farron A. Influence of glenohumeral conformity on glenoid stresses after total shoulder arthroplasty. J Shoulder Elbow Surg 2006;15:515-20. https://doi.org/10.1016/j.jse.2005.09.021
48. Walch G, Badet R, Boulahia A, Khoury A. Morphologic study of the glenoid in primary glenohumeral osteoarthritis. J Arthroplasty 1999;14:756-60.
49. Walch G, Moraga C, Young A, Castellanos-Rosas J. Results of anatomic nonconstrained prosthesis in primary osteoarthritis with biconcave glenoid. J Shoulder Elbow Surg 2012;21:1526-33. https://doi.org/10.1016/j.jse.2011.11.030
50. Walker KE, Simcock XC, Jun BJ, Iannotti JP, Ricchetti ET. Progression of glenoid morphology in glenohumeral osteoarthritis. J Bone Joint Surg Am 2018;100:49-56. https://doi.org/10.2106/JBJS.17.00064
51. Wright TW, Grey SG, Roche CP, Wright L, Flurin PH, Zuckerman JD. Preliminary results of a posterior augmented glenoid compared to an all polyethylene standard glenoid in anatomic total shoulder arthroplasty. Bull Hosp Jt Dis (2013) 2015;73(Suppl 1):S79-85.
52. Yian EH, Werner CM, Nyffeler RW, Pfirrmann CW, Ramappa A, Sukthankar A, et al. Radiographic and computed tomography analysis of cemented pegged polyethylene glenoid components in total shoulder replacement. J Bone Joint Surg Am 2005;87:1928-36. https://doi.org/10.2106/JBJS.D.02675
53. Youderian AR, Ricchetti ET, Drews M, Iannotti JP. Determination of humeral head size in anatomic shoulder replacement for glenohumeral osteoarthritis. J Shoulder Elbow Surg 2014;23:955-63. https://doi.org/10.1016/j.jse.2013.09.005